Journal of Biomolecular NMR, **16:** 245–252, 2000.
KLUWER/ESCOM

A new approach for applying residual dipolar couplings as restraints in structure elucidation

Jens Meiler[a], Niklas Blomberg[b], Michael Nilges[b] & Christian Griesinger[a]
[a]*Universität Frankfurt, Institut für Organische Chemie, Marie-Curie-Strasse 11, D-60439 Frankfurt am Main, Germany*
[b]*EMBL, Meyerhofstrasse 1, D-69012 Heidelberg, Germany*

Received 27 October 1999; Accepted 27 December 1999

Key words: protein structure determination, residual dipolar coupling

Abstract

Residual dipolar couplings are useful global structural restraints. The dipolar couplings define the orientation of a vector with respect to the alignment tensor. Although the size of the alignment tensor can be derived from the distribution of the experimental dipolar couplings, its orientation with respect to the coordinate system of the molecule is unknown at the beginning of structure determination. This causes convergence problems in the simulated annealing process. We therefore propose a protocol that translates dipolar couplings into intervector projection angles, which are independent of the orientation of the alignment tensor with respect to the molecule. These restraints can be used during the whole simulated annealing protocol.

Introduction

Residual dipolar couplings can be used to determine the orientation of an intermolecular vector in the coordinate system of the alignment tensor effected either by paramagnetic moieties of the molecule or by using diluted liquid crystals (Tolman et al., 1995; Hong et al., 1996; Bax and Tjandra, 1997; Tjandra and Bax, 1997; Wang et al., 1998; Cordier et al., 1999; Ojennus et al., 1999). Residual dipolar couplings are used in structure calculations optimizing the orientation of bond vectors with respect to the orientation of the external alignment or susceptibility tensor (Clore et al., 1998b, 1999; Ottiger et al., 1998; Bayer et al., 1999; Fischer et al., 1999; Olejniczak et al., 1999). From the distribution of the dipolar couplings it is possible to extract the size of the protein alignment tensor (Clore et al., 1998a); however, the orientation of the tensor with respect to the molecule that is defined by three Euler angles cannot be determined without structure calculation. In addition, the translation of the dipolar coupling into an orientation in the frame of the alignment tensor is ambiguous due to the fact that there is a continuum of α, β pairs for each dipolar coupling and the mirror reflection symmetry along each of the axes of the alignment tensor. A restraint based on the orientation of a vector in an alignment tensor therefore corresponds to a complicated energy hypersurface ensuing slow convergence properties of the algorithm.

To avoid convergence problems, we propose here to transform the dipolar coupling restraints into purely intramolecular projection restraints that do not require knowledge of the orientation of the molecule with respect to the alignment tensor. We demonstrate with two examples that with this implementation the convergence of the simulated annealing protocol with and without dipolar couplings is almost identical. On a model system it is shown that the precision of the structures is enhanced by the use of the dipolar couplings.

*To whom correspondence should be addressed. E-mail: cigr@org.chemie.uni-frankfurt.de

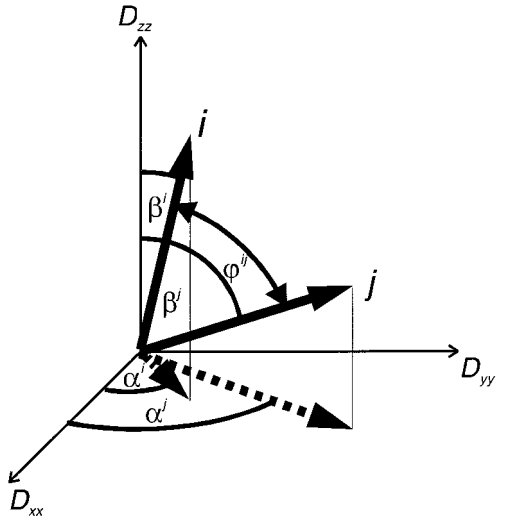

Figure 1. Two bond vectors i and j in the coordinate system of the alignment tensor (D_{xx},D_{yy},D_{zz}). The angles $\alpha^{i/j}$ and $\beta^{i/j}$ determine the projection of the vector onto the z-axis and of the x,y-component onto the x-axis of the alignment tensor, respectively. φ^{ij} determines the angle between the two vectors i and j.

Theory

In order to derive equations for the projection angles of interatomic vectors as a substitute for the orientation restraints, we introduce the coordinate system of Figure 1, in which the two vectors i and j are defined in the coordinate system of the alignment tensor with the values D_{xx}, D_{yy} and D_{zz}. Defining an axially symmetric $D_\parallel$ and a rhombic part $D_\perp$ of the tensor according to:

$$\begin{aligned} D_\parallel &= \frac{1}{3}\left(D_{zz} - \frac{D_{xx}+D_{yy}}{2}\right) \\ D_\perp &= \frac{2}{3}\left(\frac{D_{xx}-D_{yy}}{2}\right) \end{aligned} \quad (1)$$

one obtains:

$$\begin{aligned} D^i\left(\beta^i\alpha^i\right) &= D_\parallel\left(3\cos^2\beta^i - 1\right) \\ &\quad + \frac{3}{2}D_\perp\left(\cos 2\alpha^i \sin^2\beta^i\right) \end{aligned} \quad (2)$$

With an experimental set of dipolar couplings the eigenvalues of the tensor D_{xx}, D_{yy}, D_{zz} can be determined from the powder pattern of experimental couplings (Clore et al., 1998a). We now derive equations that allow the use of the dipolar couplings as restraints without the need for defining the orientation of the alignment tensor. This is done by calculation of the projection angle φ^{ij} between all pairs of internuclear vectors i and j for which dipolar couplings have been measured.

$$\cos\varphi^{ij} = \begin{pmatrix} \cos\alpha^i \sin\beta^i \\ \cos\alpha^i \sin\beta^i \\ \cos\beta^i \end{pmatrix}^T \begin{pmatrix} \cos\alpha^i \sin\beta^j \\ \cos\alpha^j \sin\beta^j \\ \cos\beta^j \end{pmatrix} \quad (3)$$

Applying Equation 2 to Equation 3 one can eliminate two angles β^i, β^j and arrive at:

$$\begin{aligned} &\cos\varphi^{ij} = \\ &\sqrt{\frac{2(3D^i - 2D_{zz} + D_{xx} + D_{yy})}{3(\frac{3}{2}(D_{xx}-D_{yy})\cos\alpha^i - 2D_{zz} + D_{xx} + D_{yy})}} \\ &\sqrt{\frac{2(3D^j - 2D_{zz} + D_{xx} + D_{yy})}{3(\frac{3}{2}(D_{xx}-D_{yy})\cos\alpha^j - 2D_{zz} + D_{xx} + D_{yy})}} \\ &\cos(\alpha_2 \pm \alpha_1) \\ &\pm\sqrt{1 - \frac{2(3D^i - 2D_{zz} + D_{xx} + D_{yy})}{3(\frac{3}{2}(D_{xx}-D_{yy})\cos\alpha^i - 2D_{zz} + D_{xx} + D_{yy})}} \\ &\sqrt{1 - \frac{2(3D^j - 2D_{zz} + D_{xx} + D_{yy})}{3(\frac{3}{2}(D_{xx}-D_{yy})\cos\alpha^j - 2D_{zz} + D_{xx} + D_{yy})}} \end{aligned} \quad (4)$$

In addition, the possible range for angle α^i is sometimes reduced by the measured coupling values:

$$if \left|\frac{6D^i + 2D_{zz} - D_{xx} - D_{yy}}{3\left(D_{xx} - D_{yy}\right)}\right| \le 1$$

$$\left\{\begin{aligned} \alpha^i_{\min} &= \tfrac{1}{2}\arccos\left(\tfrac{6D^i+2D_{zz}-D_{xx}-D_{yy}}{3(D_{xx}-D_{yy})}\right) \\ \alpha^i_{\max} &= \pi - \tfrac{1}{2}\arccos\left(\tfrac{6D^i+2D_{zz}-D_{xx}-D_{yy}}{3(D_{xx}-D_{yy}}\right) \end{aligned}\right\} \quad (5)$$

$$else \left\{\begin{aligned} \alpha^i_{\min} &= 0; \\ \alpha^i_{\max} &= \pi \end{aligned}\right\}$$

Depending on the size of the measured coupling values, the angle φ^{ij} is no longer allowed to vary in the whole interval from 0 to π. Equation 5 states that the extreme values of φ^{ij} will always be found at the extreme values for α^i and α^j. The allowed range for φ^{ij} is in addition always symmetric about $\varphi^{ij} = \pi/2$ (Figure 2). Two general possibilities are found:

one allowed range: $\varphi^{ij} \in [\epsilon_1, \pi - \epsilon_1]$
two allowed ranges: $\varphi^{ij} \in [\epsilon_1, \pi/2 - \epsilon_2]$
or $\varphi^{ij} \in [\pi/2 + \epsilon_2, \pi - \epsilon_1]$

with $\epsilon_{1,2} \in [0,\pi/2]$. The symmetry of the allowed φ^{ij} ranges is directly related to the geometric symmetries of the dipolar couplings according to Equation 2. Figure 2 shows a range for one angle φ^{ij} that has been calculated in this way.

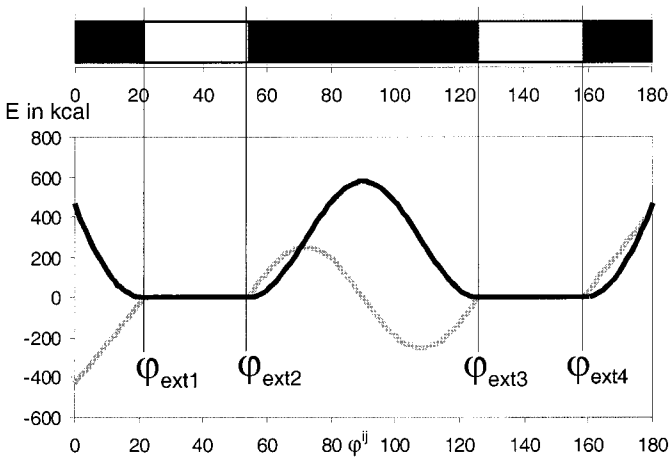

Figure 2. Potential employed to confine φ^{ij} within the allowed range (white) and exclude it from the forbidden range (black). A flat bottom potential is used for the allowed region, a parabolic potential for the margins close to *0* and π and a $\cos^2 \Delta\varphi^{ij}$ function for the inner forbidden part. The energy term used is given by the black line and its derivative (negative force) by the gray line.

Using this approach one can calculate from *n* dipolar couplings $n(n-1)/2$ ranges for angles φ^{ij}. These ranges are now free from information about tensor orientation. The translation of the dipolar couplings into intervector projection angles, i.e., the scalar product is the simplest pairwise relation between two vectors and any further more complicated vector relation yielding a scalar value can be derived from it. At the same time, the scalar product conserves all information and more complicated intervector relations are not required. This can be inferred from the following argument: If for a set of N vectors, the length of the vectors and all the mutual projection angles are known, the orientations of the vectors are uniquely defined. N vectors can be represented by N+1 atoms, where the N vectors all start from the (N+1st) atom. This set of atoms has 3(N+1) degrees of freedom. Since we know the length of the vectors (N+1) degrees of freedom and the projection angles: N(N+1)/2 degrees of freedom and subtracting 3 degrees of freedom each for rotation and translation, we find: $3(N+1)-(N+1)N/2-6-(N+1) \leq 0$ for all N. Thus, the projection angles would even overdetermine the coordinates of the vectors if they were exactly known.

To use these angle ranges φ^{ij} for structure determination, a new restraint was introduced in the X-PLOR program (Brünger, 1992). The energy function used is displayed in Figure 2 and given in Equation 6:

$$\begin{aligned}
E^{ij}_{0\rightarrow\varphi_{ext1}} &= k_1\left(\varphi^{ij}-\varphi^{ij}_{ext1}\right)^2 \\
E^{ij}_{\varphi_{ext1}\rightarrow\varphi_{ext2}} &= 0 \\
E^{ij}_{\varphi_{ext2}\rightarrow\varphi_{ext3}} &= k_2\cos^2\left(\pi\left(\frac{\varphi^{ij}-\varphi^{ij}_{ext2}}{\varphi^{ij}_{ext3}-\varphi^{ij}_{ext2}}-\frac{1}{2}\right)\right) \\
E^{ij}_{\varphi_{ext3}\rightarrow\varphi_{ext4}} &= 0 \\
E^{ij}_{\varphi_{ext4}\rightarrow 180^\circ} &= k_1\left(\varphi^{ij}-\varphi^{ij}_{ext4}\right)^2
\end{aligned} \quad (6)$$

k_1 and k_2 are the energy constants used in these implementations. Note that k_2 gives directly the height of the barriers between the two allowed φ^{ij} ranges while k_1 scales the square of the deviation from the extreme values. The two energy constants can be scaled separately during the simulated annealing protocol, which turned out to be essential as discussed below.

Results and discussion

The protocol has been applied to the protein Rhodniin, which has 103 amino acids and contains two similar folded domains of 45 amino acids and a flexible linker of 10 amino acids. A set of dipolar couplings between amide nitrogen and amide hydrogen was calculated from the known NMR structure (M. Maurer and C. Griesinger, in preparation) of the protein assuming a specific orientation of the alignment tensor. The eigenvalues were set to be $D_{zz} = 20.0$ Hz, $D_{yy} = -17.5$ Hz and $D_{xx} = -2.5$ Hz, amounting to a rhombicity of 0.5. This set of dipolar couplings is used as an *'experimental'* test set of data and the Rhodniin structure they were calculated from is called *'target structure'*.

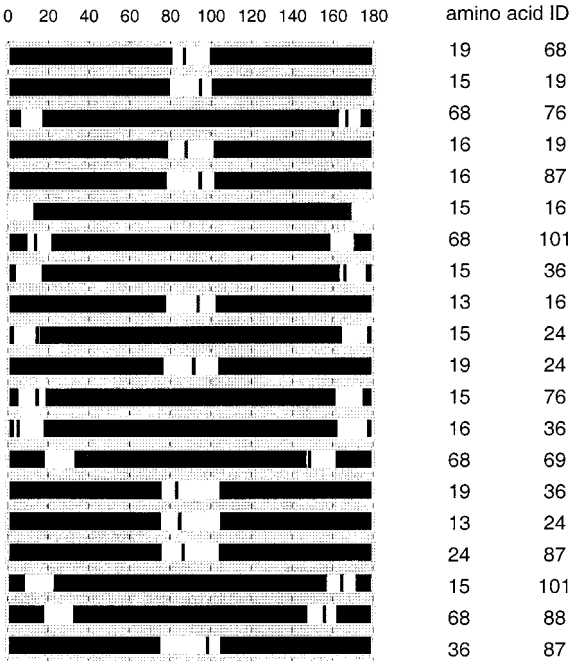

Figure 3. Allowed and forbidden ranges for the angles φ^{ij} between those N-H^N vectors that are most restricted by the dipolar couplings derived from one alignment tensor. The black bars are the φ^{ij} values of the 'target' structure of Rhodniin.

Table 1. Number of restraints that exclude a defined percentage of the possible φ^{ij} ranges

Percentage of φ^{ij} range excluded (%)	Number of restraints	Percentage of restraints (%)
0–10	802	26.18
10–20	781	22.75
20–30	736	18.92
30–40	624	14.25
40–50	494	8.51
50–60	304	5.41
60–70	213	2.86
70–80	163	0.91
80–90	67	0.38
90–100	2	0.00
Sum	4186	100.00

All NOEs used in the following calculations were put in three groups: strong NOEs < 2.5 Å, medium NOEs < 3.5 Å and weak NOEs < 5.0 Å. A flat bottom potential was used, being zero for all values smaller than the mentioned distances and quadratically increasing for larger distances.

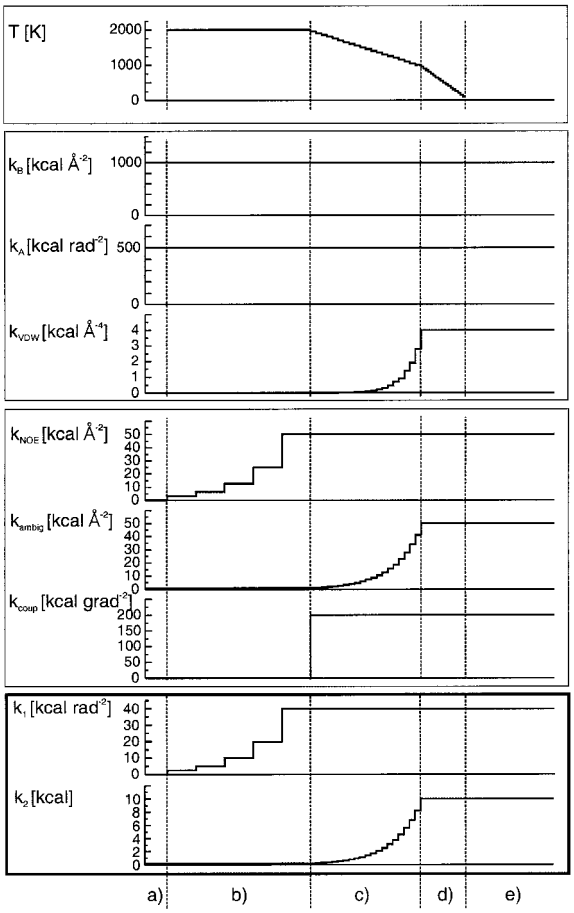

Figure 4. Time scale, temperature and size of the energy constants during the simulated annealing as used for the example Rhodniin in X-PLOR (Brünger, 1992). (a) Initial energy minimization of 50 steps is performed. (b) High temperature phase, lasting for 32.5 ps. The energy constants used for dipolar couplings k_1 are switched on together with the unambiguous NOEs. (c) First cooling phase, lasting for 25.0 ps: k_2 is switched on together with the rest of the NOE. Temperature is decreased from 2000 K to 1000 K. (d) Second cooling phase, lasting 10.0 ps. Temperature is decreased from 1000 K to 100 K. (e) Final energy minimization of 200 steps is performed using all restraints and their final force constants.

The eigenvalues of the alignment tensor were back calculated from the powder pattern of the dipolar couplings (Clore et al., 1998a) yielding $D_{zz} = 19.6$ Hz, $D_{yy} = -17.4$ Hz and $D_{xx} = -2.2$ Hz. This tensor has a slight deviation from predefined values, caused by the fact that values are extracted from a powder pattern. From the dipolar couplings more than 4000 possible φ^{ij}–angle ranges were calculated using these eigenvalues. Figure 3 shows the 20 most restricted ranges. Table 1 reports the number of φ^{ij}–angle restraints that exclude a given percentage of the possible

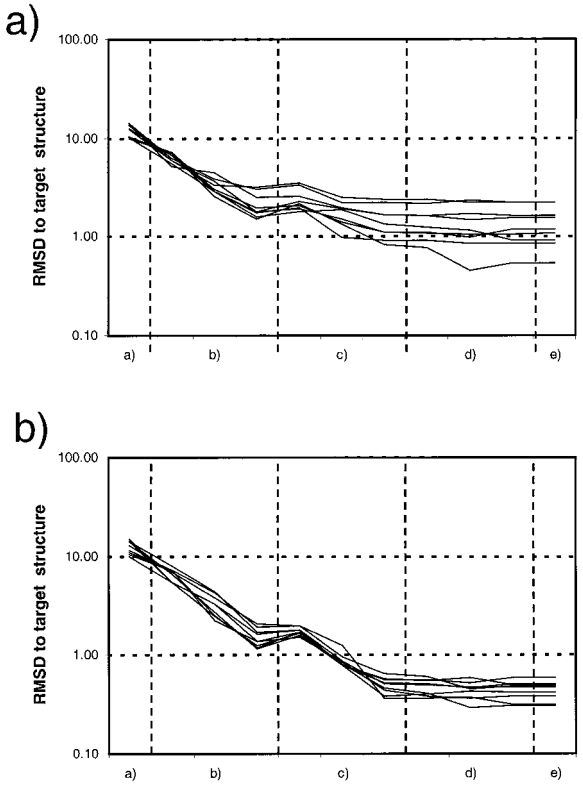

Figure 5. Logarithmic representation of rmsd to target structure during simulated annealing without (a) and with (b) the use of dipolar couplings for the N-domain of Rhodniin as a function of the sections of the SA explained in Figure 4. Best 10 out of an ensemble of 100 calculated structures. The precision and accuracy of the structure with dipolar couplings (both 0.5 Å) are higher than without (both 1.2 Å).

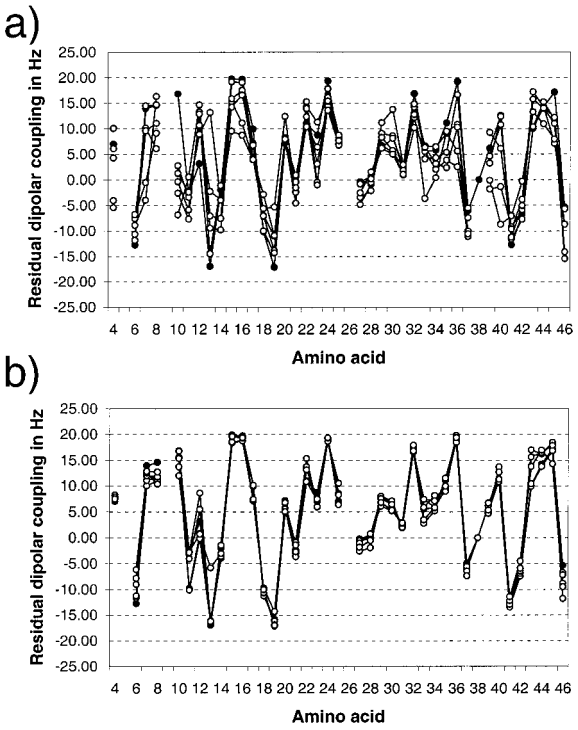

Figure 6. Couplings recalculated for the resulting structures without (a) and with (b) the restriction of the angle ranges. The normalized standard deviation (Q) decreases from 0.66 without (a) the use of the angle restraints to 0.19 with (b) the use of the angle restraints.

range from [0,π]. Since only a small part of the restraints contains most of the structural information, we find that only those 30% to 50% (depending on the data) most restricted ranges are necessary in the calculations.

k_1 and k_2 were varied between 0 kcal/mol and 200 kcal/mol and gave best results with $k_1 = 40$ kcal/mol rad^{-2} and $k_2 = 10$ kcal/mol. Figure 4 shows the scaling of the force constants used during the simulated annealing X-PLOR protocol. In order to keep the energy surface simple, only k_1 is ramped up, together with the force constant for the unambiguous NOEs in the high temperature phase. k_2 is ramped up in the first cooling phase, together with the force constant of the ambiguous NOEs. k_2 defines the height of the barrier between the two possible ranges φ^{ij}. It turns out to be essential to choose the right period in the simulated annealing protocol, when k_2 is ramped up. We find that the convergence deteriorates when k_2 is switched on too early, namely already in the high temperature phase. By contrast, the number of violated angle restraints increases when k_2 is ramped up too late, namely during the second cooling phase.

With the scaling of force constants as depicted in Figure 4, two ensembles of 100 structures were calculated with and without all angle restraints, all experimentally determined NOEs and J-coupling restraints. For the convergence, we focused on the N-terminal domain of Rhodniin. Figure 5 shows the rmsd of the heavy atoms in the N-terminal domain of the best 10 out of the 100 calculated structures to the target structure during the simulated annealing protocol with and without the angle restraints, respectively. The rmsd decreases from 1.2 Å to 0.5 Å by introducing the information derived from dipolar couplings, which is in line with previous results obtained for ubiquitin (Bax and Tjandra, 1997). In the best 10 of these structures no NOEs and between zero and three of the angle ranges are violated. Table 2 reports the energy distribution of the 100 structures. The introduction of the φ^{ij} restraints increases the mean energy of the ensemble. However, only 5 out of the 100 struc-

Table 2. Energy distribution of an ensemble of 100 structures after the simulated annealing protocol without angle restraints, with restraints and with restraints for two different tensors

Energy range (kcal)	Number of structures		
	Without dipolar restraints	With one set of dipolar restraints	With two sets of dipolar restraints
350–450	47	31	12
450–550	43	38	30
550–650	6	14	28
650–750	3	6	13
750–850	0	2	9
850–950	0	3	2
> 950	1	5 + 1	5 + 1

With the use of the dipolar restraints five structures do not converge at all. One converges, however, at 990 kcal/mol and 1100 kcal/mol, respectively.

tures do not fold to a meaningful NMR structure and have a very high energy (beyond 5000 kcal/mol) but 83 have an energy lower than 650 kcal/mol. Without the use of the couplings 96 structures have an energy below 650 kcal/mol. The agreement between the dipolar couplings and the 'experimental' restraints is very good, as is reported in Figure 6 for 5 out of the 100 structures with the lowest energy. After the simulated annealing protocol, the orientation of the tensor was optimized (Losonczi et al., 1999) using the program DipoCoup (J. Meiler, W. Peti and C. Griesinger, submitted; Meiler, 1999). All deviations are given as dipolar Q-factor (normalized standard deviation, Cornilescu et al., 1998). This factor is bigger by $\sqrt{2}$ than the R-factor (Clore and Garrett, 1999). The dipolar Q-factor is 0.19 with the use of the restraints but 0.66 without angle restraints. Small deviations can be explained with the slightly incorrect alignment tensor eigenvalues used for calculating the restraints as well as with the violation of angle ranges in some special cases. The orientation of the tensor is reproduced within $\pm 5°$.

During a second type of experiment only part of the NOEs was used to test the possibility of replacing NOE information by dipolar couplings. All NOEs containing at least one amide hydrogen were selected first. Out of this subgroup of NOEs a varying percentage of 20% to 100% was randomly selected to be used in the calculation. Amide hydrogens were chosen, since their NOEs are the first and easiest to obtain during evaluation of the spectra and are the only NOEs available in deuterated proteins. Table 3 shows the rmsd values to the target structure with respect to the amount of NOEs used for the N-domain of the protein. The structures can be determined more accurately using the angle restraints. The largest improvement is observed when 60% to 80% of the amide-to-all-proton NOEs are used. Differences are smaller if more or less than 60% to 80% of the NOEs are used. This shows that, based on a minimal amount of NOEs that define the fold, dipolar couplings improve the structure. If the number of NOEs exceeds a certain number, they define the structure so well that dipolar couplings do not improve the accuracy of the structure considerably any more. If the number of NOEs is too low the fold is no longer determined and the dipolar couplings cannot remedy this situation.

Table 3. Rmsd to target structure with and without the use of angle restraints

Percentage of NOEs used (%)	Rmsd to target structure (in Å)	
	With dipolar restraints	Without dipolar restraints
20	5.39	5.75
40	4.20	4.40
60	2.90	4.13
80	1.78	3.50
100	1.73	2.26

20%, 40%, 60%, 80% and 100% of the NOEs including at least one H^N-atom are used. All other NOEs, including ambiguous NOEs, are excluded.

A third calculation was performed to test the ability of this implementation to determine the global structure of Rhodniin. Therefore 50 structures were generated, and the orientation of the two Rhodniin domains with respect to each other was investigated. For this calculation the 500 most restricted interdomain φ^{ij} ranges as well as the 500 most restricted intradomain φ^{ij} ranges for the N-domain and the C-domain, respectively, are used. Figure 7 shows the five resulting structures with lowest energy. Three out of these five structures show the same relative orientation of the domains identical to the target structure. In the other two cases one domain is rotated by 180° around the x-axis of the alignment tensor. Due to the symmetry of the tensor, this is a valid solution. In all cases not more than five φ^{ij} ranges are slightly outside of the allowed range. Recalculating dipolar couplings from all five structures with an optimized tensor orientation shows that all five structures fulfill the dipolar coupling values.

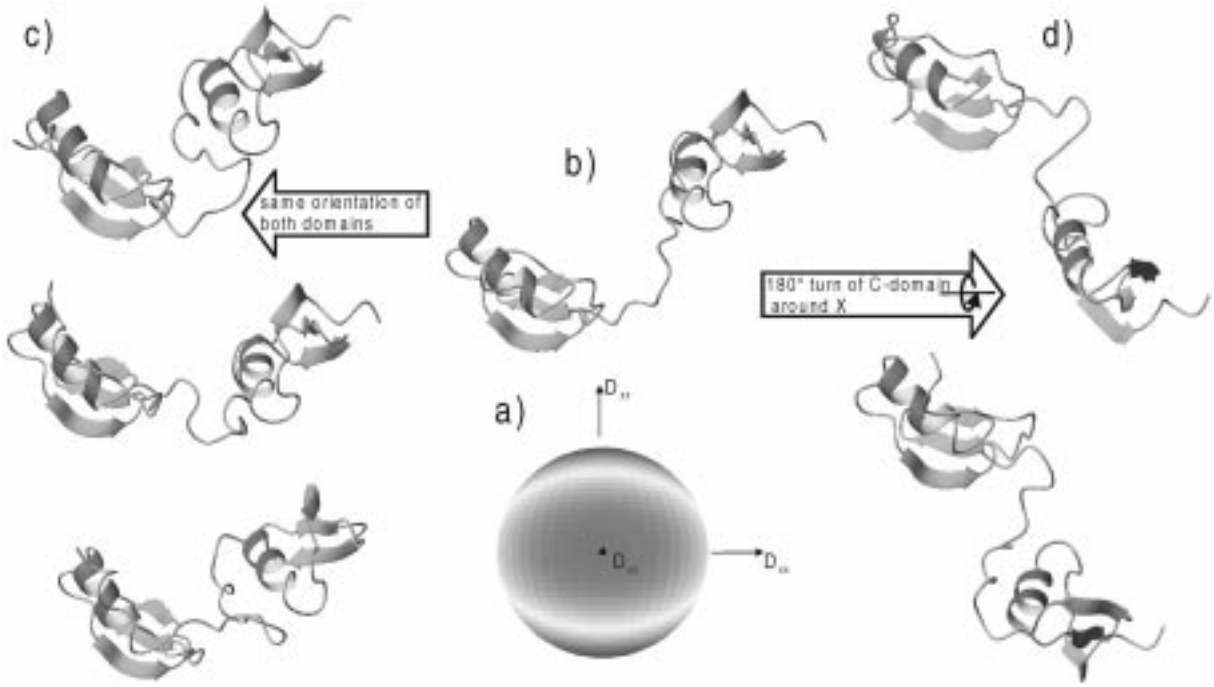

Figure 7. The relative orientation of the N- and C-domain of Rhodniin with respect to each other. The tensor (a) and the target structure (b) in the coordinate system of the tensor are shown. (c) and (d) display the best 5 out of 50 structures from the simulated annealing protocol of Figure 4. (c) The three structures with the same orientation of the domains as in the target structure are shown. (d) Two structures are obtained in which one domain is rotated by 180° about the D_{xx} axis with respect to the target structure.

To check the ability of the program to use two sets of dipolar couplings obtained with two different alignment tensors (Ramirez and Bax, 1998), a second tensor was defined, $D_{zz} = 10.0$ Hz, $D_{yy} = -6.5$ Hz and $D_{xx} = -3.5$ Hz, amounting to a rhombicity of 0.2. The orientation of the tensor with respect to the original PDB file of the target structure was changed from $(\alpha,\beta,\gamma) = (60°,135°,0°)$ for the first alignment tensor to $(\alpha,\beta,\gamma) = (120°,90°,133°)$ for the second alignment tensor. A second set of dipolar couplings was calculated and from these values derived φ^{ij} ranges were used together with the ranges depicted from the first set of dipolar couplings to recalculate the N-domain of Rhodniin.

With the use of both sets of angle restraints and the same protocol as used before, still 70 out of the 100 structures calculated have an energy lower than 650 kcal/mol. For the 10 structures with lowest energy no NOE is violated and only 0 to 10 of the angle restraints are slightly violated. The dipolar Q-factor is 0.16 for the first set of dipolar couplings and 0.14 for the second set of dipolar couplings. The rmsd of the structures to the target structure decreases also to be 0.3 Å.

In order to test the protocol with an experimental set of dipolar couplings, it was applied on a second protein. The PH domain of the protein Unc89 from *C. elegans* (residues 341 to 458) was expressed in *E. coli* and purified as described elsewhere (Blomberg et al., 2000). The domain has the native sequence with a single methionine residue added to the N-terminus. Deuterated dimethyl sulphoxide (DMSO; 15%) was added to the samples to suppress aggregation and precipitation. All NMR experiments were recorded at 303 K on a Bruker DRX600 or DRX500 spectrometer equipped with pulse field gradient triple resonance probes. The resonance-frequency assignment of the UNC-89 PH domain is deposited in the BioMagResBank (http://www.bmrb.wisc.edu, accession no. 4373). All experimental data as well as the structure determination of the protein is described and discussed elsewhere (Blomberg et al., 2000).

Residual dipolar couplings were measured for ^{1}J-NH-couplings from standard ^{15}N-HSQC experiments without decoupling in the indirect dimension. Alignment of the PH domain was achieved using DMPC/DLPC/SDS lipid bicelles (ratio 3.2:1:0.1; 5% w/v total lipid) (Losonczi and Prestegard, 1998; Ot-

tiger et al., 1998). Bicelle formation, evidenced by the observed splitting of the D_2O signal, was achieved at 298 K and the measurements of dipolar couplings were performed at 303 K. A reference spectrum was recorded with the sample in the isotropic phase at 295 K. Residues with severe overlap in the ^{15}N-HSQC spectra and those showing evidence of large mobility (elevated ^{15}N T_2/T_1 ratio or short T_2's) were excluded, yielding a total of 41 long range angular restraints.

The magnitude of the tensor components was estimated from a histogram (Clore et al., 1998a) to be $D_{zz} = 8.32$ Hz, $D_{yy} = -6.34$ Hz and $D_{xx} = -1.98$ Hz, amounting to a rhombicity of 0.35. From this data 861 φ^{ij} ranges were derived and used in the simulated annealing process. It was necessary to increase the force constants to be $k_1 = 80$ kcal rad^{-2} and $k_2 = 20$ kcal to get no more than five angle restraints slightly violated. Two ensembles with 100 structures each were calculated, one without and the second with the use of the angle restraints. The dipolar Q-factor of the experimental coupling values to those calculated from the final structures is 0.20 with the use of the restraints, but 0.79 without angle restraints. As already obtained in the calculations of Rhodniin, the energies of the structures increase about 10% using angle restraints. The converged amount of structures with and without restraints is similar to the result for Rhodniin. The rmsd for the backbone of the protein decreases from 2.70 Å without the use of the angle restraints to 2.15 Å with the use of the restraints.

Conclusions

The use of dipolar couplings as φ^{ij} restraints allows to include these experimental data from the start of the simulated annealing protocol. Moreover, with this implementation the dipolar couplings can for the first time be directly translated into intramolecular restraints without the need to orient the alignment tensor during the simulated annealing protocol. The convergence of the simulated annealing protocol is almost unchanged as compared to calculations without dipolar couplings. The calculation time increases only slightly (below 5% for these examples) by taking dipolar couplings into account.

Acknowledgements

This work was supported by the 'Fond der chemischen Industrie', the DFG and the MPG. J.M. thanks the 'Fond der chemischen Industrie' for a Kekulé-Stipendium. We thank M. Maurer, Frankfurt, for making available all the Rhodniin data. We thank W. van Gunsteren, ETH Zürich, and S. Glaser, TU München, for enlightening discussions.

References

Bax, A. and Tjandra, N. (1997) *J. Biomol. NMR*, **10**, 289–292.
Bayer, P., Varani, L. and Varani, G. (1999) *J. Biomol. NMR*, **14**, 149–155.
Blomberg, N., Sattler, M. and Nilges, M. (1999) *J. Biomol. NMR*, **15**, 269–270.
Blomberg, N., Sattler, M., Baraldi, E., Saraste, M. and Nilges, M. (2000) submitted.
Bruenger, A.T. (1992) *X-PLOR, A System for X-Ray Crystallography and NMR*, Yale University Press, New Haven, CT.
Clore, G.M., Gronenborn, A.M. and Bax, A. (1998a) *J. Magn. Reson.*, **133**, 216–221.
Clore, G.M., Gronenborn, A.M. and Tjandra, N. (1998b) *J. Magn. Reson.*, **131**, 159–162.
Clore, G.M. and Garrett, D.S. (1999) *J. Am. Chem. Soc.*, **121**, 9008–9012.
Clore, G.M., Starich, M.R., Bewley, C.A., Cai, M. and Kuszewski, J. (1999) *J. Am. Chem. Soc.*, **121**, 6513–6514.
Cordier, F., Dingley, A.J. and Grzesiek, S. (1999) *J. Biomol. NMR*, **13**, 175–180.
Cornilescu, G., Marquardt, J.L., Ottiger, M. and Bax, A. (1998) *J. Am. Chem. Soc.*, **120**, 6836–6837.
Fischer, M.W.F., Losonczi, J.A., Weaver, J.L. and Prestegard, J.H. (1999) *Biochemistry*, **38**, 9013–9022.
Hong, M., Schmidt-Rohr, K. and Zimmermann, H. (1996) *Biochemistry*, **35**, 8335–8341.
Losonczi, J.A., Andrec, M., Fischer, M.W.F. and Prestegard, J.H. (1999) *J. Magn. Reson.*, **138**, 334–342.
Losonczi, J.A. and Prestegard, J.H. (1998) *J. Biomol. NMR*, **12**, 447–451.
Meiler, J. (1999) http://krypton.org.chemie.uni-frankfurt.de/~mj/
Ojennus, D.D., Mitton-Fry, R.M. and Wuttke, D.S. (1999) *J. Biomol. NMR*, **14**, 175–179.
Olejniczak, E.T., Meadows, R.P., Wang, H., Cai, M. and Fesik, S.W. (1999) *J. Am. Chem. Soc.*, **121**, 9249–9250.
Ottiger, M., Delaglio, F., Marquardt, J.L., Tjandra, N. and Bax, A. (1998) *J. Magn. Reson.*, **134**, 365–369.
Ramirez, B. and Bax, A. (1998) *J. Am. Chem. Soc.*, **129**, 9106–9107.
Tjandra, N. and Bax, A. (1997) *Science*, **278**, 1111–1113.
Tolman, J.R., Flanagan, J.M., Kennedy, M.A. and Prestegard, J.H. (1995) *Proc. Natl. Acad. Sci. USA*, **92**, 9279–9283.
Wang, H., Eberstadt, M., Olejniczak, E.T., Meadows, R.P. and Fesik, S.W. (1998) *J. Biomol. NMR*, **12**, 443–446.